A transimpedance preamplifier using a feedforward approach for robust rejection of DC photogenerated currents

Ettore Masetti, Stefano Cattini and Luigi Rovati

COLLECTIONS

F   This paper was selected as Featured

View Online   Export Citation   CrossMark

ARTICLES YOU MAY BE INTERESTED IN

A transimpedance preamplifier using a feedforward approach for robust rejection of DC photogenerated currents 🄵

Ettore Masetti,[a] 🆔 Stefano Cattini, 🆔 and Luigi Rovati 🆔

AFFILIATIONS

Dipartimento di Ingegneria Enzo Ferrari. University of Modena and Reggio Emilia, Modena (MO) 41125, Italy

[a]Author to whom correspondence should be addressed: ettore.masetti@unimore.it

ABSTRACT

The preamplifier proposed in this paper is designed to extract weak variable photogenerated signals from a high-level continuous background ensuring low noise and high transimpedance gain. An efficient cancellation of the DC component directly at the photodetector output, exploiting a feedforward approach, allows us to properly amplify the variable signal components of interest avoiding saturation of the preamplifier. Furthermore, the large transimpedance gain allows for minimizing the effects of the noise introduced by the following stages on the signal processing chain. In the paper, we present the proposed approach and a possible circuit realization with a signal AC/DC ratio as small as 1/1000 ensuring low noise, high gain, and a considerable bandwidth. The realized preamplifier offers a Noise Equivalent Power $NEP \simeq 1.12$ nW, an in-band transimpedance gain of 4.4 MΩ, and a wide bandwidth from about 1 Hz up to 100 kHz, making it suitable for use in several applications both in biomedical and industrial fields.

Published under an exclusive license by AIP Publishing. https://doi.org/10.1063/5.0130239

I. INTRODUCTION

Detection of weak signals encoded in optical fields is a common problem in many applications. In most cases, the transduction of these signals is performed by a photodiode, which generates a photocurrent proportional to the optical power impinging on its sensitive area. Due to their low cost and easy implementation, transimpedance amplifiers (TIAs) are the most common circuit used for converting photogenerated currents into voltages.

Even if the implementation of a TIA stage requires very few electronic components, its design requires great attention, especially when dealing with weak signals spread over a wide frequency band. In these cases, when designing the readout electronics, a fundamental figure of merit to be considered is the output signal-to-noise ratio. In particular, in a good preamplifier design, the impact of the noise introduced by the conditioning electronics should be negligible with respect to the photon shot noise of the detector.[1] A very useful metric to isolate the noise performances of the front-end electronics from the input optical power is the so-called Noise-Equivalent-Power (NEP), which determines the smallest signal that can be correctly detected, given the intrinsic noise of the detector. It is known that a low-noise front-end design requires a high TIA gain, which unavoidably compromises the detection bandwidth.[2]

The preamplifier design becomes even more critical when, as happens in some applications, a huge constant ambient (or background) light is superimposed on the weak optical signal of interest. The large background photogenerated current yields a fairly large loss in the output voltage swing for the useful AC component, which enormously limits the achievable TIA gain by worsening the noise performance of the entire front-end electronics.

The need of rejecting the DC component of the photogenerated current to ensure adequate amplification of the AC part is common in many applications. A first important example concerns the optical feedback in the cavity of coherent or low-coherent sources, i.e., a self-mixing laser diode or a self-mixing superluminescent diode.[3,4] This optical approach is mainly used to perform interferometric measurements. In the classic self-mixing configuration, the monitor photodiode, housed inside the optical source case is used to detect the beating between the interfering electric fields. The modulation depth is usually very small; therefore, a strong DC component is superimposed on the useful signal. Furthermore, if the self-mixing

approach is used to obtain Doppler signals, the TIA frequency band must be sufficiently wide.

For example, in the application we proposed for blood flow measurements, a flat bandwidth from 1 Hz to 100 kHz was required.[5] In inertial rotation-sensing applications, fiber-optic gyroscopes based on Sagnac interferometers allow precise measurement of the rotation rate.[6] In these systems, one or more photodiodes acquire the optical signal that contains an AC signal carrying useful rotation rate information and an unwanted DC component proportional to the laser source intensity. The AC signal amplitude corresponding to a rotation rate is usually very small, e.g., 1 pA for an angular rate of 1 deg/h, and a wide bandwidth (in the order of 1 MHz) is required. In addition, in this case, the unwanted DC signal represents a problem in the preamplification and information extraction phases. Another measuring system with an extremely small AC/DC ratio is the photoplethysmography. This medical device performs non-invasive monitoring of the pulsatile blood volume and oxygenation in living tissue. The pulsatile component of the optical signal is completely immersed in the background due to the backscattering of the tissues interposed between the optical probe and the blood vessels. Nevertheless, in this type of measurement, the background DC component is equally essential for retrieving significant vital parameters.[7] Another example in the biomedical field is the optrodes in the context of neural recording.[8] The weak time-varying useful signal is also in this case superimposed on an ideally time-invariant high-level component.

To our knowledge, to date, three main approaches have been proposed to reject the DC component of the photodiode photocurrent: (i) the TIA amplifies both DC and AC components, and the DC component is then filtered out in the next stages;[9] (ii) the TIA transfer function is designed to cut the DC signal components while maintaining adequate gain for the AC component;[10] and (iii) an Offset Detector Circuit (ODC) connected to the TIA output generates a signal, which is then subtracted from the photogenerated signal.[6,10]

The first solution is undoubtedly the simplest but, as anticipated before, the DC component yields a fairly large loss in the output voltage swing for the useful AC component and, consequently, the TIA gain is bounded from above, which results in worse noise performance of the entire front-end electronics.

The basic idea of the second solution is to exploit reactive components (capacitors or inductors) to block or cancel the effect of the DC component of the photogenerated signal. The solution that exploits a decoupling capacitor directly at the entrance of the TIA stage was analyzed in detail by Wei *et al.*[11] as a photodiode zero-mode working condition. However, this very simple circuit topology provokes a non-linear operation of the photodiode and requires certain precautions in its use. First, the lower cut-off frequency depends on the photodiode junction capacitance. To overcome this problem, large capacities can be used, e.g., Wei *et al.* proposed 1 mF capacitance to obtain a lower cut-off frequency as low as 1 Hz not depending on the photodiode junction capacitance, but this obviously implies large circuit sizes and non-idealities depending on the type of decoupling capacitor used. Another important aspect that limits its use is that the higher the DC component of the photogenerated current, the smaller the TIA gain. This is because under high light level injection, the photodiode reaches the nonlinear region and the I–V curves are compressed. In some applications,

this could nullify the advantage in terms of voltage output swing for the AC component due to decoupling. As an alternative to the use of the decoupling capacitor, Rovati and Docchio[2] proposed to use an inductor instead of the TIA feedback resistor. This solution guarantees the classic photoconductive operation of the photodiode, but since the impedance of the inductor is directly proportional to the frequency, the TIA gain at zero frequency is null. The aforementioned circuit, proposed as a differentiator stage, can easily be used as a TIA by adding a second integrator stage to obtain a constant gain in the frequency range of interest. Although this simple circuit topology has considerable advantages in terms of noise, it has the big limitation of requiring large inductors, which, in addition to their overall dimensions, are critical due to possible coupling with disturbances.

The use of an ODC has recently been proposed by Zhang *et al.* for a differential configuration.[6] They modified a TIA feedback tee-network by introducing a DC cancellation loop based on a Deboo integrator circuit. This stage senses the total TIA output and its output is used to counteract the TIA output offset caused by the photogenerated DC component. This interesting solution requires careful design and trade-offs among bandwidth, stability, noise, gain, and matching conditions determined by the value of each resistor in the tee-network. In particular, the feedback gain must be carefully chosen to ensure stability. It is also known that the tee-network reduces the effects of parasitic capacitances but worsens the signal-to-noise ratio.

Starting from the last approach, in this paper, we propose to exploit the same photodiode signal to generate a compensation current to null the DC component of the photogenerated signal; still maintaining the possibility of retrieving the DC information, useful in some biomedical applications, such as photoplethysmography. The basic idea is to do not sense the TIA output but the photocurrent, which is normally dispersed to ground to generate the compensation offset that, exploiting a feedforward approach, is used to cancel the unwanted component of the photogenerated current before the preamplification. This approach allows leaving the TIA feedback circuit topology unaltered and offers an undoubted advantage in terms of noise by acting directly on the TIA input and avoiding the tee-network, and in terms of circuit stability. The proposed solution features an extremely high AC gain and a complete rejection of the DC counterpart, still offering a wide bandwidth and excellent noise performances. In the following, Sec. II starts with a description of the working principle of the proposed circuital solution. Circuit considerations, transfer function, and noise performance analysis are addressed in this section. Section III presents the experimental results with a prototype designed and realized for self-mixing applications. The presented TIA can properly work with AC/DC ratios as small as 1/1000 offering a high AC gain, i.e., 4.4 MΩ, and a large bandwidth from less than 1 Hz up to 100 kHz. Conclusions are drawn in Sec. IV discussing possible limitations and improvements.

II. CIRCUIT DESIGN AND THEORETICAL ANALYSIS

The operating principle of the proposed circuit approach is to exploit both the photodiode anode and cathode outputs to cancel the photogenerated DC component before the preamplification. Normally, in low-noise detection circuits of optical signals

at medium–low frequency, the photodiode is unbiased. This allows reduction of the shot noise due to the junction reverse current at the expense of a greater value of the junction capacitance and, in turn, a slower photodiode response. Since the preamplifier circuit usually consists of a transimpedance stage, the photodiode is connected between the virtual ground of an operational amplifier and the ground. Hence one of the two generated photocurrents, i.e., anode and cathode currents, is not used but simply dispersed to ground. Our idea is, therefore, to acquire this current with another transimpendence stage and exploit it for our purposes.

In the following, we assume the photogenerated current to consist of two contributions:

$$I_{PD} = I_{AC} + I_{DC}, \tag{1}$$

where I_{AC} includes all the spectral components of I_{PD} with the frequency between f_L and f_H and represents the useful component of the signal. I_{DC} includes all the spectral components of I_{PD} with the frequency lower than f_L, which do not contain useful information and must be rejected.

A. Functional block diagram

The block diagram of the proposed electronic configuration is shown in Fig. 1. The photogenerated current I_{PD} feeds both the main TIA and a secondary TIA in the feed-forward circuit. The secondary TIA filters out the AC component of I_{PD} amplifying I_{DC}. Thus, the Voltage-Controlled current Generator (VCG) generates the likelihood estimation $\widetilde{I_{DC}}$ of I_{DC}. Therefore, if we assume that $\widetilde{I_{DC}} = I_{DC}$, then the main TIA only amplifies the component of interest (I_{AC}) of the photogenerated signal. Note that the proposed scheme uses a feedforward technique; therefore, it requires an initial gain adjustment of the feedforward network to ensure the rejection condition. After this initial tuning, the feedforward network ensures the correct tracking and cancellation of the DC component avoiding, unlike approaches that exploit feedback schemes,[6] critical stability conditions. Thus, the signal spectral components of interest can be precisely defined without worrying about possible feedback instabilities.

B. Circuit transfer function

According to the block diagram in Fig. 1, the current generated by the feedforward block can be expressed as
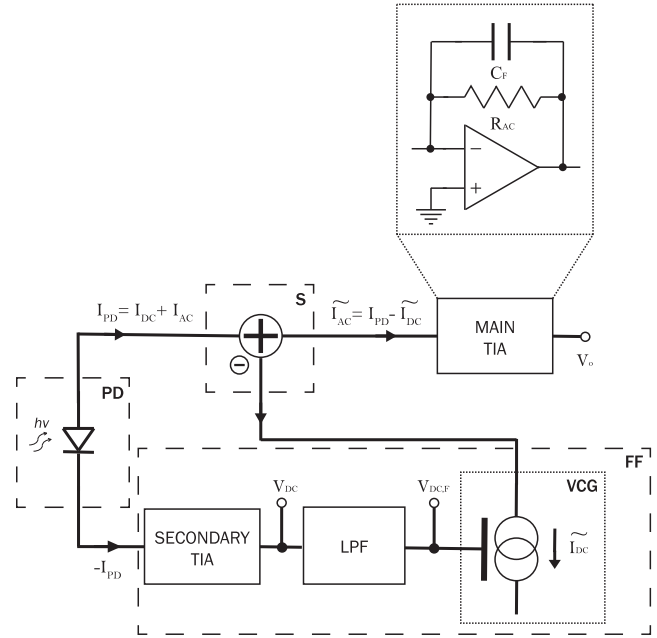
$$\widetilde{I_{DC}} = g_m \cdot V_{DC,F} = g_m \cdot I_{PD} \cdot \mathscr{G}_{DC}, \tag{2}$$

where g_m is the transconductance of the VCG and $\mathscr{G}_{DC}$ takes into account the transfer functions of the secondary TIA and low-pass filter (LPF). Therefore, the network output voltage is

$$V_o = \left(I_{AC} + I_{DC} - \widetilde{I_{DC}} \right) \cdot \mathscr{G}_{AC}, \tag{3}$$

where $\mathscr{G}_{AC}$, in the simple circuit configuration in Fig. 1 (main TIA), it is

$$\mathscr{G}_{AC} = \frac{R_{AC}}{1 + s \cdot \tau_{AC}}. \tag{4}$$

FIG. 1. Functional block diagram of the preamplifier. The PD block represents the input photodiode of the overall preamplifier. The photogenerated current is exploited using both terminals of the photodiode; in one direction, it feeds the FeedForward (FF) section, whereas in the other branch, it is the input of the summation block S. The FF block is composed of a secondary TIA, a Low-Pass Filter (LPF) and a Voltage-Controlled current Generator (VCG). The LPF is a third order Butterworth filter with cut-off frequency f_L. The VCG produces an estimate $\widetilde{I_{DC}}$ of the photodiode DC current component I_{DC}. However, the main TIA and secondary TIA blocks consist in standard transimpedance amplifiers.

Time constant $\tau_{AC} = R_{AC} \cdot C_F = \frac{1}{2 \cdot \pi \cdot f_H}$ is defined to satisfy the circuit bandwidth requirements. Two fundamental components of the output signal are, therefore, identifiable,

$$V_o = I_{AC} \cdot \mathscr{G}_{AC} + \left(I_{DC} - g_m \cdot I_{PD} \cdot \mathscr{G}_{DC} \right) \cdot \mathscr{G}_{AC}. \tag{5}$$

The first addend represents the component of the photogenerated signal of interest, while the second is the term that must be canceled by the feedforward circuit. Hence, the gain $\mathscr{G}_{DC}$ feedforward circuit must be tuned for the following relation to be satisfied:

$$\mathscr{G}_{DC} = \frac{1}{g_m} \cdot \frac{I_{DC}}{I_{PD}} = \frac{1}{g_m} \cdot \frac{1}{1 + \frac{I_{AC}}{I_{DC}}}. \tag{6}$$

The spectral characteristics of the two gains $\mathscr{G}_{AC}$ and $\mathscr{G}_{DC}$ can then be designed for a precise selection of the I_{PD} spectral components of interest (I_{AC}), and the one to be rejected (I_{DC}). Basically, the transfer function $\mathscr{G}_{DC}$ has to ensure that the following conditions are met:

$$\begin{cases} I_{AC} \to 0, & \mathscr{G}_{DC} \to \frac{1}{g_m} & f \ll f_L, \\ I_{DC} \to 0, & \mathscr{G}_{DC} \to 0 & f \gg f_L. \end{cases} \tag{7}$$
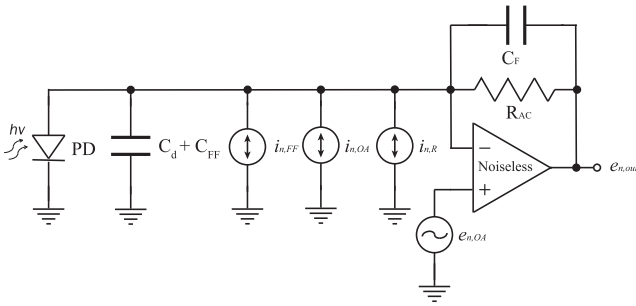
FIG. 2. Schematic representation of the main TIA, modeled with a noiseless operational amplifier and external current and voltage noise sources. The capacitor C_T represents the overall input capacitance of the main TIA, in parallel to the input photodiode. The main noise sources are given by the current noise produced by the feedforward network ($i_{n,FF}$), the current and voltage noise models due to the operational amplifier ($i_{n,OA}$ and $e_{n,OA}$), and the current noise related to the feedback resistor ($i_{n,R}$).

C. Noise considerations

Compared to the classic TIA configuration, the proposed circuit introduces a single additional source of noise due to the noise superimposed on the $\widetilde{I_{DC}}$ current. In Fig. 2, the main sources of noise are schematically represented.

Equivalent input noise generators $i_{n,OA}$ and $e_{n,OA}$ model the noise characteristics of the operational amplifier, while $i_{n,R}$ describes the thermal noise contribution introduced by the feedback resistor R_{AC}. In addition to these three components, always present in the standard TIA configuration, $i_{n,FF}$ models the noise generator introduced by the feedforward network. The capacitance $C_T = C_d + C_{FF}$ takes into account the photodetector capacitance, i.e., C_d, and the capacitance introduced by the feedforward circuit, i.e., C_{FF}. A careful circuit design ensures that the former is dominant over the latter, and thus, $C_T \simeq C_d$.

Hence, the noise at the circuit output is

$$v_{n,o} = \left(i_{n,OA} + i_{n,R} + i_{n,FF}\right) \cdot \frac{R_{AC}}{1 + s \cdot \tau_{AC}} + \left(1 + \frac{s \cdot \tau_d}{1 + s \cdot \tau_{AC}}\right) \cdot e_{n,OA}, \tag{8}$$

where $\tau_{AC} = R_{AC} \cdot C_F$ and $\tau_d = R_{AC} \cdot C_T \simeq R_{AC} \cdot C_d$.

As shown in Fig. 3, in order to compare the noise introduced by the TIA with the photogenerated signal, it is useful to model the preamplifier as a noiseless block and refer to its noise in terms of total equivalent noise current,

$$i_{n,T} = \frac{v_{n,o}}{\mathcal{G}_{AC}} = i_{n,OA} + i_{n,R} + i_{n,FF} + \frac{e_{n,OA}}{R_{AC}} \cdot (1 + s \cdot (\tau_{AC} + \tau_d)). \tag{9}$$
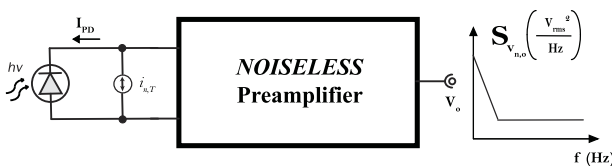
FIG. 3. Preamplifier noise model: noiseless block with the equivalent input referred to as a noise current generator $i_{n,T}$ at the input. $i_{n,T}$ takes into account for all the circuit noise contributions.

In terms of one-sided noise power spectral density, the input noise current generator $i_{n,T}$ is thus described by

$$S_{i_{n,T}} = S_{i_{n,OA}} + S_{i_{n,R}} + S_{i_{n,FF}} + \frac{S_{e_{n,OA}}}{R_{AC}^2} \cdot \left(1 + (2\pi \cdot f \cdot (\tau_{AC} + \tau_d))^2\right), \tag{10}$$

where $S_{(\cdot)}$ represents the one-sided noise power spectral density of the noise generator $(\cdot)$.

To calculate the one-sided current input noise power spectral density $S_{i_{n,T}}$, starting from the datasheet of the operational amplifier, we have reconstructed the noise power spectra of the generators $i_{n,OA}$ and $e_{n,OA}$ shown in Fig. 2.

The power spectral density of $i_{n,R}$, can be calculated as[12]

$$S_{i_{n,R}} = \frac{4 \cdot k_B \cdot T}{R_{AC}}, \tag{11}$$

where k_B is the Boltzmann constant and $T = 300$ K is the operating temperature.

While for the $i_{n,FF}$ generator, it is possible to assume that the main contribution is due to the JFET (Junction-gate Field Effect Transistor), the narrow bandwidth of the feedforward network makes the other contributions less significant.

Thus, according to Ref. 12, $S_{i_{n,FF}}$ can be estimated as

$$S_{i_{n,FF}} \simeq 4 \cdot k_B \cdot T \cdot \left(\frac{2}{3} g_m\right), \tag{12}$$

where g_m is the JFET transconductance. Note that the used JFET has an I_{DSS} much higher than the maximum expected $\widetilde{I_{DC}}$, allowing it to operate far from the zero gate voltage condition, which corresponds to a smaller g_m value, and a lower noise level.

In conclusion, a fundamental figure of merit to evaluate the noise performances of our preamplifier is the Noise-Equivalent-Power (NEP), which represents the input power that provides a unitary signal-to-noise ratio at the output. For an input photodiode, the NEP is defined as the ratio of its equivalent input noise current to the responsivity and can be computed as[13]

$$NEP = \frac{1}{\sigma} \cdot \sqrt{\int_0^{f_H} S_{i_{n,T}} \, df}, \tag{13}$$

where σ is the photodetector responsivity.

III. CIRCUIT IMPLEMENTATION AND EXPERIMENTAL RESULTS

To experimentally verify the actual performances achievable by the solution proposed in Sec. II A, we designed and realized a TIA stage designed for the Self-Mixing Superluminescent Diode (SM-SLD) interferometer for flow measurements, as proposed in our previous paper.[14] In this Doppler velocimeter, a SM-SLD is exploited to detect the beating signal. The photodiode on the back-facet of a commercial SLD is used to detect the light scattered by the flowing particles. Thanks to the low coherence length of the optical source, the system allowed us to measure the velocity profile of the flowing scatterers even in turbid and absorbing media.

The TIA bandwidth required for this system obviously depends on the frequencies of the Doppler signal and therefore, in turn, on the range of flows of interest. In the experimental setup that we

proposed,[14] the measurement was aimed at determining the flow velocity profile into a capillary glass duct (R = 0.4 mm) with flow velocity up to about 200 mm/s. This required the TIA bandwidth to be around 100 kHz.

The reflections of the optical components and capillary walls, and the scattering of particles that did not contribute to the interference phenomenon made the ratio between the AC and DC components of the photogenerated signal extremely critical, i.e., in the order of 1/1000.

Hence, this Doppler velocimeter is a typical application where our circuit proposal can find application. According to the main block diagram described in the previous sections, we realized the circuit shown in Fig. 4. It is possible to notice a direct correspondence of the main building blocks of the circuit with respect to the functional block diagram (Fig. 1): (i) the photodiode (PD), (ii) the current summation node (S), (iii) the feedforward circuit (FF), and (iv) the main transimpedance amplifier (M-TIA). The feedforward block was designed to produce a precise replica of the DC component of the photogenerated current I_{DC}; it consists of (i) a secondary transimpedance amplifier (S-TIA), (ii) a third order Butterworth Low Pass Filter (BW-LPF), and (iii) the Voltage Controlled current Generator (VCG). The S-TIA is a simple transimpedance amplifier with an in-band gain of $R_{DC} = 4.7$ kΩ and a cut-off frequency of $f_L = 1/(2\pi R_{DC}C_{DC}) = 1$ Hz. A low-noise JFET input operational amplifier (LF347BN, by Texas Instruments) was used to minimize its input noise contribution.

The output V_{DC} of this stage accurately tracks the DC component of the photogenerated current that must be rejected. Residuals of AC components ($f > f_L$) included in this tracking voltage were filtered out by the third order Butterworth low-pass filter having the same cut-off frequency (f_L) (UAF42, by Texas Instruments). This filter offers a unitary gain in-band flat response and a very steep (−60 dB/dec) roll-off.

The voltage $V_{DC,F}$ drives the VCG, which consists of a first non-inverting stage including an offset adjustment potentiometer (i.e.,

R_{offset}) and a low-noise current source for floating loads. The current $\widetilde{I_{DC}}$ is generated by this stage thanks to the negative feedback of the operational A_{VCG-2} (LF347BN, by Texas Instrument), which biases the gate of the n-channel JFET (MMBFJ113, by ON Semiconductor) so that its drain current is

$$\widetilde{I_{DC}} = \frac{V_{DC,F} - V_{ref}}{R_{pd}}. \tag{14}$$

The feedforward network must produce a current $\widetilde{I_{DC}}$ very close to the DC component of the photogenerated current I_{DC}. The aforementioned condition is obtained by correctly tuning the feedforward network, which consists of two main steps:

- The SLD is turned OFF, so the monitor photodiode is not exposed to any light source, hence the input of the TIA is null. The offset resistor R_{offset} is tuned in order to obtain a voltage $V_{DC,J}$ that is exactly equal to V_{ref}. This step allows to compensate for any bias introduced by the feedforward network.
- The SLD is biased to a defined current I_{LD}, so the monitor photodiode is exposed to a constant amount of light. The adjusting resistor R_{adj} is regulated in order to guarantee the current matching condition of the feedforward network. In other words, R_{adj} is finely adjusted to obtain $\widetilde{I_{DC}} \approx I_{DC}$; hence, $V_o|_{DC} \approx 0$.

The summation node S accomplishes the role of subtracting $\widetilde{I_{DC}}$ to the photodiode current I_{PD}, providing to the M-TIA only the AC component of the photogenerated current I_{AC}. The M-TIA was realized with a high in-band gain $R_{AC} = 4.4$ MΩ and a cut-off frequency $f_H = 1/(2 \cdot \pi \cdot R_{AC} \cdot C_F) = 150$ kHz. The M-TIA was implemented using a High-Precision Low-Noise operational amplifier (OPA228, by Texas Instruments).
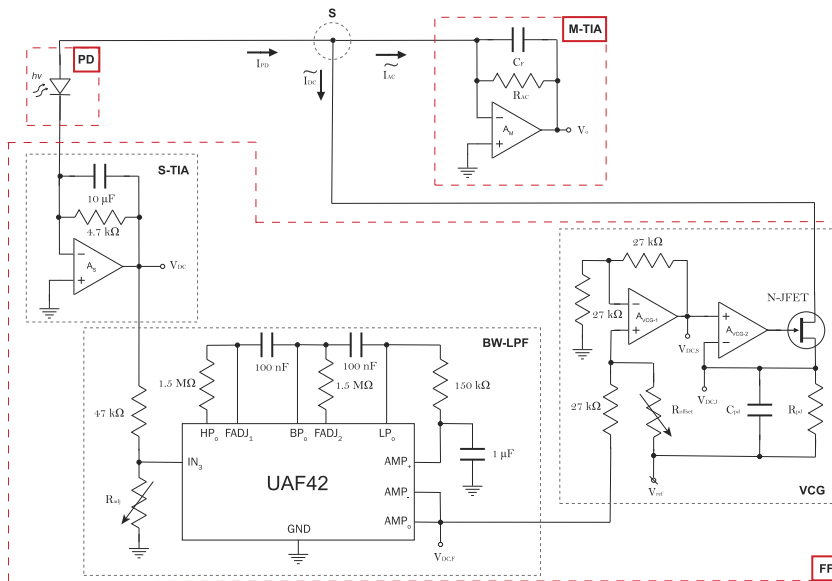
FIG. 4. TIA circuit implementation for our Doppler velocimeter: PD: photodiode, FF: feedforward circuit, and M-TIA: main transimpedance amplifier. The feedforward network is composed of a secondary transimpedance amplifier (S-TIA), a Butterworth Low-Pass Filter (BW-LPF) and a Voltage Controlled current Generator (VGC).

A. Experimental transfer function

The experimental setup shown in Fig. 5 was realized to verify the TIA transfer function.

The SLD (SLD-381-MP-DBUT-SM-PD-830, Superlum) was polarized by a commercial laser diode controller (LDC205C, Thorlabs) and thermally controlled by the thermoelectric controller TEC (TED200C, Thorlabs). The monitor photodiode detecting the optical power at the output of the cavity back-facet was connected to our TIA. The SLD was then biased at a constant current $I_{LD,0}$ = 95 mA and kept at a fixed temperature T_0 = 25 °C. The Dynamic Signal Analyzer (DSA) (SR785, Stanford Research Systems) was used to drive the laser diode controller and to acquire the M-TIA output voltage, whereas the Digital Storage Oscilloscope (DSO) was used to monitor the S-TIA DC output.

The DSA generated the sweep frequency input stimulus V_d applied to the laser diode controller, which in turn, modulated the SLD current around the bias point. The transimpedance function has to be inferred from the measured global transfer function (GTF) expressed as follows:

$$\mathbf{GTF}(s) = \frac{V_o}{V_d} = \xi \cdot \mathbf{CC}|_{I_{LD,0}} \cdot \mathbf{R_T}(s), \quad (15)$$

where $\xi = \frac{dI_{LD}}{dV_d}$ = 0.05 A/V is the laser diode controller (LDC) modulation coefficient and $\mathbf{CC}|_{I_{LD,0}} = \frac{dI_{PD}}{dI_{LD}}\Big|_{I_{LD,0}}$ = 0.011 93 is the coupling coefficient between the photodiode current and the SLD current.

After 30 min warm-up time, the TIA under test working condition was set: a single tone signal V_d (amplitude 10 mV and frequency 1 kHz) was generated and the TIA offset and feedforward setting point were adjusted. Following this, the DSA was set to generate a sweep frequency V_d from 0.1 Hz to 100 kHz (the maximum frequency for the instrument) with 400 points/decade, so the **GTF** was acquired. To obtain such a resolution over a wide spectral range, the measurement was carried out in several steps over reduced
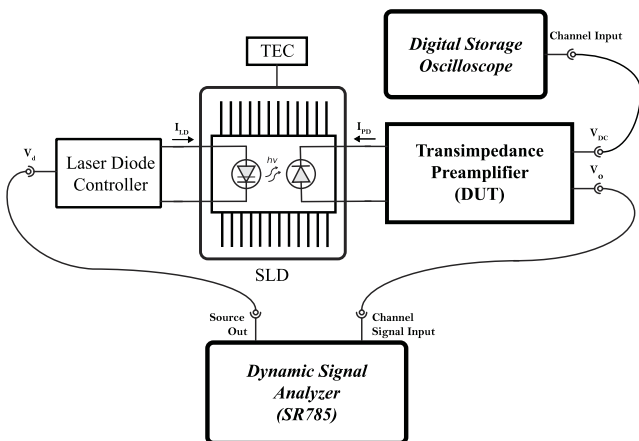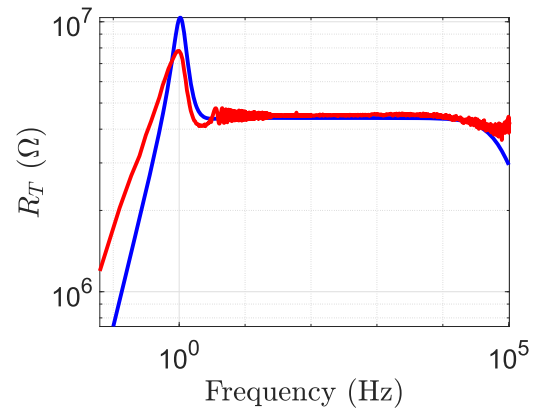
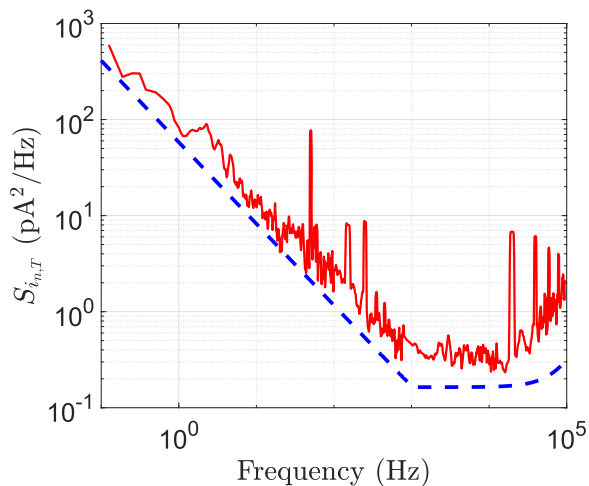**FIG. 6.** Experimental (red) and theoretical (blue) TIA transimpedance transfer functions.

spectral intervals. According to Eq. (15), the experimental TIA transfer function $\mathbf{R_T}(s)$ was calculated. Figure 6 shows the so obtained TIA transfer function $\mathbf{R_T}(s)$. The TIA theoretical transfer function obtained analytically from Eq. (5) is also shown in the same figure. Note the good agreement between the experimental and theoretical TIA transfer functions. As expected, the in-band transimpedance gain is 4.4 MΩ except for the R_{AC} tolerance, whereas the −3 dB bandwidth is (1 Hz, 100 kHz). The spectral 1 Hz overshoot is mainly due to the Butterworth filter transfer function.

B. Noise performances

According to Eq. (13), the TIA noise performances can be described in terms of NEP. To measure the one-sided noise power spectral density of the TIA output $S_{v_{n,o}}$, we used the same setup shown in Fig. 5 disconnecting the SLD photodiode from the TIA and setting the DSA for power spectrum measurements. After 30 min of warm-up time, the TIA one-sided noise power spectral density was acquired. By dividing this power spectrum by the square of the experimental transfer function, the current input noise power spectral density was then computed.

Figure 7 shows the so obtained TIA current input referred to noise power spectral density $S_{i_{n,T}}$. The theoretical current input noise power spectral density obtained analytically from Eq. (13) is also shown in the same figure. Note the good agreement between the experimental and theoretical spectra. For low frequencies, the 1/f components of the parallel noise generators, i.e., $i_{n,OA}$, $i_{n,R}$, $i_{n,FF}$, are dominant. The effect of the series component of the input noise, i.e., $e_{n,OA}$, is clearly visible in the rise of the spectral density of noise power at frequencies greater than 10 kHz. The spectrum demonstrates that the optimum spectral range in which this circuit can provide the best noise performance is 1 to 10 kHz. Nevertheless, assuming that our application requires a spectral range from 1 Hz to 100 kHz, we proceeded with the calculation of the NEP according to Eq. (13).

The experimental noise power spectral density $S_{i_{n,T}}$ was numerically integrated over the spectral range (0.1 Hz, 100 kHz) to approximate the integral in Eq. (13). While, for the value of responsiveness, neither from the SLD datasheets nor from the manufacturer, we

FIG. 5. Transfer function measuring setup: LDC: laser diode controller, SLD: superluminescent diode, TEC: thermo-electric controller, DSO: digital storage oscilloscope, TIA: transimpedance preamplifier (DUT: device under test), DSA: digital signal analyzer.

FIG. 7. Equivalent input current noise power spectral density of the preamplifier. The blue curve represents the theoretical power spectral density, computed considering the TIA main noise sources. The red plot represents the experimental power spectral density, obtained by applying the experimental TIA transfer function (red curve of Fig. 6) to the measured output noise power spectral density.

were able to obtain the exact value of the photodiode responsivity σ. Nevertheless, we know that it is a standard uncoated silicon photodiode; thus, we can assume, with good approximation, a value of responsivity $\sigma = 0.55$ A/W at the SLD peak wavelength $\lambda_0 = 830$ nm.

Therefore, according to Eq. (13), the TIA NEP can be approximated as

$$NEP \simeq \frac{1}{0.55 \text{ A/W}} \cdot \sqrt{\int_{0.1 \text{ Hz}}^{100 \text{ kHz}} S_{i_{n,T}} \, df} = 1.12 \text{ nW}. \quad (16)$$

IV. CONCLUSIONS

The proposed circuit approach exploits the well-known feedforward technique. In particular, the commonly not used signal coming directly from the photodiode is exploited to create a rejection signal for the unwanted photogenerated components. In the paper, this technique was used to extract weak variable photogenerated signals from a high-level continuous background.

Since the components to be rejected are well-known, a feedforward circuit offers some advantages with respect to negative feedback solutions. The first and most important advantage is that the feedforward network does not affect the stability, sensitivity, and overall gain of the main TIA. Moreover, the negative feedback circuits take corrective actions based on the main TIA output that could be affected by electrical disturbances, whereas the proposed feedforward circuit directly exploits the photodiode current taking corrective actions without possible errors due to electrical disturbances. On the other hand, the main drawback of the feedforward circuit is that, unlike feedback, it is not self-correcting. For this reason, great care must be taken to avoid possible drifts of the feedforward stage, these are reflected directly on the output generating errors, i.e., in our circuit, unwanted output offsets.

The circuit example reported in the paper demonstrates how an accurate design allows achieving a good rejection of the DC components, ensuring the possibility of precisely defining the circuit transfer function without paying attention to network stability issues. Furthermore, it has been shown how excellent performances in terms of noise can be achieved by operating the unwanted component rejection directly on the input of the main TIA.

AUTHOR DECLARATIONS

Conflict of Interest

The authors have no conflicts to disclose.

Author Contributions

Ettore Masetti: Conceptualization (equal); Data curation (lead); Formal analysis (lead); Investigation (equal); Methodology (equal); Project administration (equal); Software (lead); Validation (lead); Writing – original draft (equal). **Stefano Cattini**: Conceptualization (equal); Investigation (equal); Methodology (equal); Project administration (equal); Resources (equal); Supervision (equal); Writing – original draft (supporting). **Luigi Rovati**: Conceptualization (equal); Formal analysis (equal); Funding acquisition (lead); Investigation (equal); Methodology (equal); Project administration (lead); Resources (lead); Supervision (equal); Validation (equal); Writing – original draft (equal).

DATA AVAILABILITY

The data that support the findings of this study are available from the corresponding author upon reasonable request.

REFERENCES

[1] W. Bowden, A. Vianello, and R. Hobson, "A low-noise resonant input transimpedance amplified photodetector," Rev. Sci. Instrum. **90**, 106106 (2019).

[2] L. Rovati and F. Docchio, "Low-noise differentiator preamplifier for photogenerated signals," Rev. Sci. Instrum. **70**, 2169–2170 (1999).

[3] G. Giuliani, M. Norgia, S. Donati, and T. Bosch, "Laser diode self-mixing technique for sensing applications," J. Opt. A: Pure Appl. Opt. **4**, S283–S294 (2002).

[4] S. Cattini and L. Rovati, "A review on guided optical feedback in superluminescence diodes for metrological purposes," J. Lightwave Technol. **39**, 3771–3780 (2020).

[5] L. Di Cecilia, S. Cattini, F. Giovanardi, and L. Rovati, "Single-arm self-mixing superluminescent diode interferometer for flow measurements," J. Lightwave Technol. **35**, 3577–3583 (2017).

[6] S. Zhang, C. Zhang, X. Pan, and N. Song, "High-performance fully differential photodiode amplifier for miniature fiber-optic gyroscopes," Opt. Express **27**, 2125–2141 (2019).

[7] N. Stuban and M. Niwayama, "Optimal filter bandwidth for pulse oximetry," Rev. Sci. Instrum. **83**, 104708 (2012).

[8] A. Al Abed, H. Srinivas, J. Firth, F. Ladouceur, N. H. Lovell, and L. Silvestri, "A biopotential optrode array: Operation principles and simulations," Sci. Rep. **8**, 2690–2716 (2018).

[9] N. A. Lockerbie and K. V. Tokmakov, "A low-noise transimpedance amplifier for the detection of "Violin-Mode" resonances in advanced Laser Interferometer Gravitational wave Observatory suspensions," Rev. Sci. Instrum. **85**, 114705 (2014).

[10] A. Pullia and F. Zocca, "Low-noise current preamplifier for photodiodes with DC-current rejector and precise intensity meter suited for optical light spectroscopy," in *IEEE Nuclear Science Symposuim and Medical Imaging Conference* (IEEE, 2010), pp. 1343–1345.

[11] Y. Wei, T. Lehmann, L. Silvestri, H. Wang, and F. Ladouceur, "Photodiode working in zero-mode: Detecting light power change with DC rejection and AC amplification," Opt. Express **29**, 18915–18931 (2021).

[12] G. Vasilescu, *Electronic Noise and Interfering Signals: Principles and Applications* (Springer, Berlin, Germany, 2005).

[13] S. Donati, *Photodetectors: Devices, Circuits and Applications*, 2nd ed. (Wiley, Hoboken, NJ, 2021).

[14] L. Rovati, S. Cattini, and N. Palanisamy, "Measurement of the fluid-velocity profile using a self-mixing superluminescent diode," Meas. Sci. Technol. **22**, 025402 (2011).